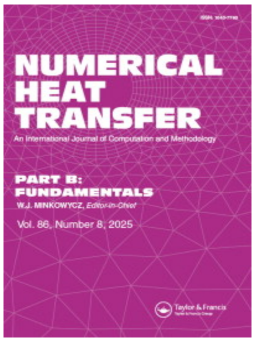

Taylor & Francis
Taylor & Francis Group

Numerical Heat Transfer, Part B: Fundamentals

An International Journal of Computation and Methodology

ISSN: 1040-7790 (Print) 1521-0626 (Online) Journal homepage: www.tandfonline.com/journals/unhb20

Reduction and estimation of discretization error using repeated Richardson extrapolation: A study involving two-phase flow problems in porous media

Marcelo Henrique Sabatini, Marcio Augusto Villela Pinto, Marcio André Martins, Michely Laís de Oliveira & Sandro Rodrigues

To cite this article: Marcelo Henrique Sabatini, Marcio Augusto Villela Pinto, Marcio André Martins, Michely Laís de Oliveira & Sandro Rodrigues (15 Jul 2025): Reduction and estimation of discretization error using repeated Richardson extrapolation: A study involving two-phase flow problems in porous media, Numerical Heat Transfer, Part B: Fundamentals, DOI: 10.1080/10407790.2025.2530192

To link to this article: https://doi.org/10.1080/10407790.2025.2530192

Published online: 15 Jul 2025.

NUMERICAL HEAT TRANSFER, PART B: FUNDAMENTALS
https://doi.org/10.1080/10407790.2025.2530192

Reduction and estimation of discretization error using repeated Richardson extrapolation: A study involving two-phase flow problems in porous media

Marcelo Henrique Sabatini[a,b], Marcio Augusto Villela Pinto[c], Marcio André Martins[a], Michely Laís de Oliveira[d], and Sandro Rodrigues[a]

[a]Department of Mathematics, State University of Centro-Oeste, Guarapuava, Paraná, Brazil; [b]Graduate Program in Numerical Methods in Engineering, Federal University of Paraná, Curitiba, Paraná, Brazil; [c]Department of Mechanical Engineering, Federal University of Paraná, Curitiba, Paraná, Brazil; [d]Research Group on Multigrid Methods, Federal University of Paraná, Curitiba, Paraná, Brazil

ABSTRACT

This study analyzes the efficiency of Repeated Richardson Extrapolation (RRE) as an alternative for reducing and estimating discretization error (E_h) in the numerical resolution of the one- and two-dimensional two-phase flow problem in porous media. The numerical solution was obtained using the finite volume method (FVM) in space and the implicit Euler method for time discretization. For linearization, we employed the modified Picard method, and to solve the linear equations system, we used the Gauss-Seidel solver coupled with the multigrid method to accelerate the convergence of the iterative process. The variables of interest analyzed were the wetting and non-wetting pressures located at the central point of the domain. The results indicate that the employed methodology was suitable, with an increase in the accuracy level of numerical solutions from 10^{-3} to 10^{-14}, and additionally, accurate estimates for E_h were obtained.

ARTICLE HISTORY
Received 1 May 2024
Revised 6 September 2024
Accepted 30 September 2024

KEYWORDS
Discretization error; error estimator; finite volume method; Richardson extrapolation; two-phase flow

1. Introduction

Numerical verification in Computational Fluid Dynamics (CFD) is a well-established field where the focus lies on the level of accuracy and reliability of numerical solutions. In this sense, high-order methods play an important role. A comparison based on counting operations is proposed in Art_Huerta2013 [1] as an evaluation tool of the computational performance of high-order methods. The tests showed that, for implicit solvers, high-order methods are more efficient than linear ones and that the optimal order is linear only for the case of element-by-element operations with cubic dependence on the degrees of freedom. In Art_Tonicello2024 [2], a high-order numerical approach based on the discontinuous Galerkin method was proposed for the simulation of two-phase flows. Numerical experiments involving viscous effects, gravitational forces, and surface tension are carried out to evaluate the developed methodology.

Other techniques are also used to increase the accuracy of the solutions. In this context, the Richardson extrapolation technique, originally proposed by Art_Richardson1927 [3], deserves special attention. Applying it recursively significantly optimizes its effectiveness, a technique referred to as Repeated Richardson Extrapolation (RRE) [4–6]. In this context, studies report the effectiveness of using the Richardson Extrapolation Method (RRE) in obtaining numerical solutions with

CONTACT Marcelo Henrique Sabatini msabatini@unicentro.br Department of Mathematics, State University of Centro-Oeste, Guarapuava, Paraná 85040-167, Brazil.

Nomenclature

Alphabetic Letters	
E_h	Discretization error
E_m	Discretization error with repeated Richardson extrapolation
F_α	Source term of phase α
g	Grid level
G	Number of grids used
$\mathbf{g}$	Gravitational acceleration vector
h	Space between the grid control volumes
K	Absolute permeability
$k_{r\alpha}$	Relative permeability of phase α
L	Spatial domain lenght
m	Extrapolation level
N_t	Number of time steps
N_x	Number of spatial discretization volumes in the x direction
N_y	Number of spatial discretization volumes in the y direction
p	Fluid pressure
p_c	Capillary pressure
p_E	Effective order
p_L	Asymptotic order
p_U	Apparent order
$\mathbf{q}$	Volumetric flow vector
S	Saturation
U_{pm}	Richardson's estimator with repeated Richardson extrapolation
$U_{p_{mc}}$	Corrected U_{pm}
Greek Letters	
α	Fluid phase
δp	Pressure correction
λ_α	Fluid mobility of phase α
μ	Fluid viscosity
ρ	Fluid density
τ	Number of time steps
$\Theta(U)$	Effectiveness of an error estimate
Φ	Porosity of the medium
Ω	Continuous domain
Ω^{h_1}	Coarse grid
Ω^{h_2}	Fine grid
Ω^{h_3}	Superfine grid

high accuracy. Art_Ertuk2005 [7] used two levels of Richardson Extrapolation (RE) in a two-dimensional cavity flow, achieving sixth-order accuracy. Art_Rahul2006 [8] investigated the precision of one-sided numerical solutions using the Finite Difference Method, reaching fourth-order accuracy by applying RRE with three distinct meshes. In CFD, Art_Marchi_Germer2013 [9] evaluated the use of RRE in reducing discretization errors in CFD for schemes from first to third order accuracy, managing to improve precision and achieving an order of precision greater than 18, highlighting the second-order central difference scheme as the most effective. Subsequent studies continued to explore the efficiency of RRE. Art_Marchi_Novak2013 [10] demonstrated that the technique could significantly reduce discretization error in solutions of the 2D Laplace equation, achieving an accuracy order of approximately 19 with reduced processing time and memory usage. Similarly, Art_AbdelMigid2017 [11] applied RRE to solve the Navier-Stokes equations for incompressible flows, raising the accuracy from second to sixth order.

However, it is important to note that few results are available in the literature for the class of problems associated with flow in porous media. An investigation into the application of RRE in the domain of poroelasticity was conducted by Art_Rodrigues2022 [12]. They demonstrated the efficiency of a methodology involving polynomial interpolation and optimization to improve accuracy in poroelasticity problems, revealing that the direct application of RRE to extreme variables is not effective, but that methodological adjustments can significantly increase the precision of numerical solutions. Their findings demonstrated a decrease in discretization errors and a notable enhancement in numerical solution accuracy.

Remark 1. The RRE increases the order of accuracy with each level of extrapolation and is a post-processing technique, therefore incurring no additional cost to generate the necessary solutions. Some high-order methods can increase the complexity of numerical schemes [1,2]. For example, in Art_Silva2021 [13] two high-order schemes (Compact-4 and Exponential-4) were evaluated and combined with RRE to achieve high order. Both studied schemes generated matrices with 9 diagonals in 2D problems, while the classical CDS-2 generated matrices with 5 diagonals.

Numerical simulations of flow in porous media are prominent in engineering problems such as oil and natural gas extraction, hydrology, soil and rock mechanics, among others [14–16]. In Art_Karimi-Fard2004 [17], a discrete fracture model compatible with reservoir simulators was developed. The method is applicable for two- and three-dimensional systems. The technique has been shown to be capable of determining effective fault-zone properties in large-scale simulations. An implicit adaptive scheme was developed in Art_Wang_Golfier2022 [18] to simulate fluid flow in a fractured vuggy porous medium in a complex geometry, usind a preconditioner to improve convergence. This method has low computational cost and good convergence performance. A model of flow in porous media containing fractures or deformation bands of high or low permeability is presented in Art_Karimi-Fard2016 [19]. Their methodology includes fine- and coarse-grid discretization. As an application, the production of gas from naturally fractured formations with low permeability was considered getting highly accurate solutions. In another study Art_Wang_Wang2022 [20] presented a method for seepage in 3D heterogeneous porous media. A mesh strategy was proposed to discretize the complex domain. Hydraulic properties is investigated to show the difference between fractures and inclusions.

For the study of multiphase problems, various mathematical models are employed, depending on factors like saturation, pressure, and relative permeability. A widely used technique for formulating these models is the mixed pressure-saturation formulation [21] or even the pressure-pressure formulation [22]. Regardless of how these models are formulated, they lead to the generation of highly nonlinear coupled systems of partial differential equations (PDE).

In this work, we study a problem involving the flow of two incompressible and immiscible fluids using the mixed pressure-saturation formulation. However, after linearization, the system is rewritten with the pressures as the primary variables. We employ the finite volume method (FVM) to discretize the spatial aspects of the PDE system, employing the centered difference scheme (CDS) and the implicit Euler method for temporal discretizations. In handling the resulting nonlinear system, we rely on the modified Picard linearization method as described by Art_Celia1992 [23]. The coupled Gauss-Seidel method [24] is used to solve the generated linear system. To accelerate the convergence of this system, we employ the multigrid method [25–27], commonly used to solve large-scale systems or general problems [28–35]. In this work, the variables of interest analyzed were the pressures in each of the wetting (w) and non-wetting (n) phases located at the central point of the domain. The results suggest that the employed methodology holds promise for enhancing the accuracy of numerical solutions in multiphase flow problems within porous media, particularly when considering the solutions obtained using RRE. Regarding estimates for discretization error, we found that the corrected Richardson estimator stood out for its accuracy and reliability.

The rest of the paper is organized as follows: in Section 2, we present the mathematical and numerical model; in Section 3, we outline the basic concepts of the multigrid method; in Sections 4 and 5, we provide the foundation for error analysis; in Section 6, we present the variable type based on grid refinement and show the results; in Section 7, we present the conclusions.

2. Mathematical formulation

2.1. Mathematical model

The governing equations for one-dimensional two-phase flow in porous media are modeled by a system of PDE that can be written as [21]:

$$\frac{\partial(\rho_\alpha \theta_\alpha)}{\partial t} + \nabla \cdot (\rho_\alpha \mathbf{q}_\alpha) = F_\alpha, \quad \text{em} \quad \Omega \times I. \tag{1}$$

In this context, the domain $\Omega \subset \mathbb{R}^+$, is defined, where $x \in \Omega = [0, L]$, $I = [0, T]$ represents a given time interval with T being the final time. The variables $\alpha = w, n$ denote the fluid phases (where w represents the wetting phase, and n represents the non-wetting phase). Additionally, ρ_α represents the density, $\theta_\alpha = \Phi S_\alpha$, where Φ is the porosity, and S_α is the saturation. Furthermore, $\mathbf{q}_\alpha$ is the volumetric flux vector, and F_α represents the source term, all related to phase α. The volumetric flux is determined by the generalized Darcy's law for the multiphase case, expressed as:

$$\mathbf{q}_\alpha = -\lambda_\alpha K(\nabla p_\alpha - \rho_\alpha \mathbf{g}), \tag{2}$$

where $\lambda_\alpha = \frac{k_{r\alpha}}{\mu_\alpha}$ represents mobility, $k_{r\alpha} = k_{r\alpha}(S_\alpha)$ is the relative permeability, μ_α is viscosity, K is the intrinsic permeability tensor [21], p_α is the pressure, all related to phase α, and $\mathbf{g}$ is the gravitational acceleration vector. Substituting Eq. (2) into Eq. (1), assuming incompressibility and a gravitational acceleration vector equal to zero, we have the simplified equation:

$$\frac{\partial(\theta_\alpha)}{\partial t} - \nabla \cdot (\lambda_\alpha K \nabla p_\alpha) = \frac{F_\alpha}{\rho_\alpha}. \tag{3}$$

Rewriting the equation for the wetting and non-wetting phases, considering $K_\alpha = k_{r\alpha} K$ and recalling that $\lambda_\alpha = \frac{k_{r\alpha}}{\mu_\alpha}$, we have

$$\frac{\partial \theta_w}{\partial t} - \nabla \cdot \left(\frac{K_w}{\mu_w} \nabla p_w \right) = \frac{F_w}{\rho_w}, \tag{4}$$

$$\frac{\partial \theta_n}{\partial t} - \nabla \cdot \left(\frac{K_n}{\mu_n} \nabla p_n \right) = \frac{F_n}{\rho_n}. \tag{5}$$

In addition to these differential equations, we have auxiliary relationships [21]: capillary pressure $p_c = p_n - p_w$ and saturation $S_w + S_n = 1$, thus, $\theta_w + \theta_n = \Phi$.

As boundary conditions, we have $p_\alpha(0, t)$ e $p_\alpha(L, t)$, $t > 0$, which are prescribed values. To complete the mathematical formulation, an initial condition must be provided, so $p_\alpha(x, 0) = p_\alpha^0$, where p_α^0 is a prescribed value of the pressure variable.

In this work, we used the analytical solution proposed by Thesis_Illiano2016 [36]. In that problem, Illiano considers the mixed pressure-saturation formulation $(\overline{p}, S_w)$, where $\overline{p} = \frac{p_w + p_n}{2}$, and proposes the analytical solution $f(x, t) = \overline{p}(x, t) = S_w(x, t) = xt(1 - x)$, defined in the domain $\Omega \times I = [0, 1] \times [0, 1]$, with initial and boundary conditions $f(x, 0) = f(0, t) = f(1, t) = 0$. To obtain an elliptic system (where it is known that the multigrid method works well), we made some modifications to the system generated by the mixed pressure-saturation formulation to rewrite it in terms of p_n and p_w variables.

Thus, some adjustments were necessary to use p_w and p_n instead of $\overline{p}$. Given that capillary pressure is given by $p_c = p_w - p_n$, we obtain

$$p_w = \overline{p} - \frac{1}{2} p_c \tag{6}$$

and

$$p_n = \overline{p} + \frac{1}{2} p_c, \tag{7}$$

where $p_c(S_w) = 1 - \frac{1}{2} S_w^2$. Since $\theta_\alpha = \Phi S_\alpha$, it follows that $\theta_w = \Phi\sqrt{2 - 2p_c}$ and $\theta_n = \Phi - \theta_w$, implying that $C_w = \frac{\partial \theta_w}{\partial p_c} = -\frac{\Phi}{\sqrt{2 - 2p_c}}$, for $p_c \neq 1$. With these expressions, we find the source terms

$$F_w = -\frac{1}{2} \rho_w \left[2\phi(x - 1)x + K_w \lambda_w t(6tx^2 - 6tx + t - 4) \right], \tag{8}$$

$$F_n = \frac{1}{2}\rho_n\left[2\phi(x-1)x + K_n\lambda_n t(6tx^2 - 6tx + t - 4)\right]. \tag{9}$$

2.2. Numerical model

We begin with the temporal discretization using the Implicit Euler method [37] and then employ the modified Picard linearization method [23]. We denote $n+1$ as the current time level, $k+1$ as the current iteration of linearization, and $\tau = \frac{T}{N_t}$ as the size of the time steps, where N_t is the number of time steps.

Then, the temporal discretization and linearization of Eqs. (4) and (5), respectively, for the wetting and non-wetting phases, are given by:

$$\frac{\theta_w^{n+1,k+1} - \theta_w^n}{\tau} - \frac{\partial}{\partial x}\left[\frac{K_w^{n+1,k}}{\mu_w}\frac{\partial}{\partial x}(p_w^{n+1,k+1})\right] = \frac{F_w^{n+1,k}}{\rho_w}, \tag{10}$$

$$\frac{\theta_n^{n+1,k+1} - \theta_n^n}{\tau} - \frac{\partial}{\partial x}\left[\frac{K_n^{n+1,k}}{\mu_n}\frac{\partial}{\partial x}(p_n^{n+1,k+1})\right] = \frac{F_n^{n+1,k}}{\rho_n}, \tag{11}$$

and then,

$$\begin{aligned} &C_w^{n+1,k}\frac{\delta p_n^{n+1,k+1} - \delta p_w^{n+1,k+1}}{\tau} - \frac{\partial}{\partial x}\left[\frac{K_w^{n+1,k}}{\mu_w}\frac{\partial}{\partial x}(\delta p_w^{n+1,k+1})\right] \\ &= \frac{\partial}{\partial x}\left[\frac{K_w^{n+1,k}}{\mu_w}\frac{\partial}{\partial x}(p_w^{n+1,k})\right] + \frac{F_w^{n+1}}{\rho_w} - \frac{\theta_w^{n+1,k} - \theta_w^n}{\tau}, \end{aligned} \tag{12}$$

$$\begin{aligned} &-C_w^{n+1,k}\frac{\delta p_n^{n+1,k+1} - \delta p_w^{n+1,k+1}}{\tau} - \frac{\partial}{\partial x}\left[\frac{K_n^{n+1,k}}{\mu_n}\frac{\partial}{\partial x}(\delta p_n^{n+1,k+1})\right] \\ &= \frac{\partial}{\partial x}\left[\frac{K_n^{n+1,k}}{\mu_n}\frac{\partial}{\partial x}(p_n^{n+1,k})\right] + \frac{F_n^{n+1}}{\rho_n} - \frac{\theta_n^{n+1,k} - \theta_n^n}{\tau}, \end{aligned} \tag{13}$$

where $C_w = \frac{\partial\theta_w}{\partial p_c} = -\frac{\partial\theta_n}{\partial p_c}$, $K_\alpha^{n+1,k} = K\lambda_\alpha$ and $\delta p_\alpha^{n+1,k+1} = p_\alpha^{n+1,k+1} - p_\alpha^{n+1,k}$.

Next, we discretize the spatial domain using the FVM. For this, we consider that our domain is a line segment with a length of L, and the uniform grid, $\{(x_i)/x_i = \left(i-\frac{1}{2}\right)h, i = 1, \ldots, N_x\}$, where $h = \frac{L}{N_x}$ is the distance between the points of the spatial discretization, and N_x is the number of spatial volumes.

We will present the development of discretization involving only the equation for the wetting phase, w, and considering the internal volumes. The procedure for the non-wetting phase, n, is analogous.

By integrating Eq. (12) over each control volume (CV), we obtain

$$\begin{aligned} &\int_{CV}\left\{C_w^{n+1,k}\frac{\delta p_n^{n+1,k+1} - \delta p_w^{n+1,k+1}}{\tau} - \frac{\partial}{\partial x}\left[\frac{K_w^{n+1,k}}{\mu_w}\frac{\partial}{\partial x}(\delta p_w^{n+1,k+1})\right]\right\} dV \\ &= \int_{CV}\left\{\frac{\partial}{\partial x}\left[\frac{K_w^{n+1,k}}{\mu_w}\frac{\partial}{\partial x}(p_w^{n+1,k})\right] + \frac{F_w^{n+1}}{\rho_w} - \frac{\theta_w^{n+1,k} - \theta_w^n}{\tau}\right\} dV. \end{aligned}$$

By applying Gauss's Divergence Theorem [38], calculating the integrals, approximating values at faces for pressures and their corrections with their nodal values, reconfiguring the resultant equation to isolate the variable δp_w, and replicating this procedure for the non-wetting phase, we obtain the following linear system which must be solved for each linearization step

$$\begin{pmatrix} A_w & B \\ B & A_n \end{pmatrix}\begin{pmatrix} \delta p_w \\ \delta p_n \end{pmatrix} = \begin{pmatrix} f_w \\ f_n \end{pmatrix}, \tag{14}$$

in which

$$A_\alpha = \begin{pmatrix} bc & & & & & & \\ (a_\alpha)_{i-1} & (a_\alpha)_i & (a_\alpha)_{i+1} & & & & \\ & (a_\alpha)_{i-1} & (a_\alpha)_i & (a_\alpha)_{i+1} & & & \\ & & \ddots & \ddots & \ddots & & \\ & & & (a_\alpha)_{i-1} & (a_\alpha)_i & (a_\alpha)_{i+1} & \\ & & & & (a_\alpha)_{i-1} & (a_\alpha)_i & (a_\alpha)_{i+1} \\ & & & & & & bc \end{pmatrix},$$

$$B = \begin{pmatrix} bc & & & & & & \\ & c_i & & & & & \\ & & c_i & & & & \\ & & & \ddots & & & \\ & & & & c_i & & \\ & & & & & c_i & \\ & & & & & & bc \end{pmatrix},$$

where bc represents boundary conditions, and

$$\begin{aligned}
(a_\alpha)_i &= -(C_w^{n+1,k})_i + \frac{\tau}{h^2\mu_\alpha}\left[(K_\alpha^{n+1,k})_{i+\frac{1}{2}} + (K_\alpha^{n+1,k})_{i-\frac{1}{2}}\right],\\
(a_\alpha)_{i+1} &= -\frac{\tau}{h^2\mu_\alpha}(K_\alpha^{n+1,k})_{i+\frac{1}{2}},\\
(a_\alpha)_{i-1} &= -\frac{\tau}{h^2\mu_\alpha}(K_\alpha^{n+1,k})_{i-\frac{1}{2}},\\
(b)_i &= (C_w^{n+1,k})_i,\\
(F_\alpha)_i &= \frac{\tau}{h^2\mu_\alpha}(K_\alpha^{n+1,k})_{i+\frac{1}{2}}(p_\alpha^{n+1,k})_{i+1} - \frac{\tau}{h^2\mu_\alpha}\left[(K_\alpha^{n+1,k})_{i+\frac{1}{2}} + (K_\alpha^{n+1,k})_{i-\frac{1}{2}}\right](p_\alpha^{n+1,k})_i +\\
&\quad \frac{\tau}{h^2\mu_\alpha}(K_\alpha^{n+1,k})_{i-\frac{1}{2}}(p_\alpha^{n+1,k})_{i-1} + \frac{\tau}{\rho_\alpha}(F_\alpha)_i^{n+1,k} - (\theta_\alpha^{n+1,k})_i + (\theta_\alpha^n)_i,
\end{aligned}$$

where $(K_\alpha^{n+1,k})_{i+\frac{1}{2}}$ and $(K_\alpha^{n+1,k})_{i-\frac{1}{2}}$ represent the conductivity at the faces of each volume for each phase, calculated as the arithmetic average. For discretization at the boundaries, we use the ghost volumes technique [39]. For the Dirichlet boundary condition at $i = 1$, we have

$$\begin{aligned}
(a_\alpha)_1 &= -(C_w^{n+1,k})_1 + \frac{\tau}{h^2\mu_\alpha}\left[(K_\alpha^{n+1,k})_{\frac{3}{2}} + 2(K_\alpha^{n+1,k})_{\frac{1}{2}}\right],\\
(a_\alpha)_2 &= -\frac{\tau}{h^2\mu_\alpha}(K_\alpha^{n+1,k})_{\frac{3}{2}},\\
(a_\alpha)_0 &= 0,\\
(b)_1 &= (C_w^{n+1,k})_1,\\
(F_\alpha)_1 &= \frac{\tau}{h^2\mu_\alpha}(K_\alpha^{n+1,k})_{\frac{3}{2}}(p_\alpha^{n+1,k})_2 - \frac{\tau}{h^2\mu_\alpha}\left[2(K_\alpha^{n+1,k})_{\frac{3}{2}} + (K_\alpha^{n+1,k})_{\frac{1}{2}}\right](p_\alpha^{n+1,k})_1 +\\
&\quad \frac{2\tau}{h^2\mu_\alpha}(K_\alpha^{n+1,k})_{\frac{1}{2}}(p_\alpha)_{bc} + \frac{\tau}{\rho_\alpha}(F_\alpha)_1^{n+1,k} - (\theta_\alpha^{n+1,k})_1 + (\theta_\alpha^n)_1,
\end{aligned}$$

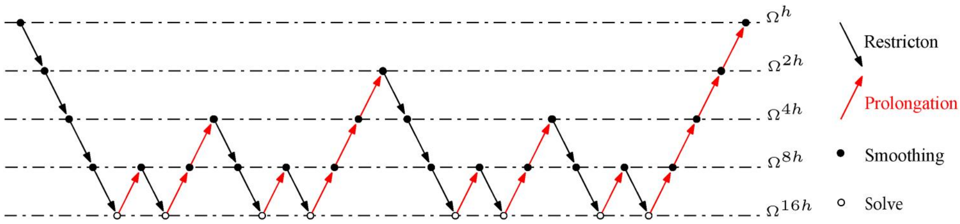

Figure 1. Representation of the multigrid W-cycle with 5 grids.

where $(p_\alpha)_{bc}$ is the boundary condition for the pressure of phase α applied at $i = 1$. The procedure is analogous to the other boundary.

3. Solver of large systems using multigrid method

The multigrid method is a numerical technique for iteratively solving systems of equations obtained by discretizing a differential equation. The method was originally proposed by Art_ Fedorenko1964 [40], showing that the convergence speed when using the multigrid technique is better than that of pure iterative methods (without the use of multigrid), which are referred to as singlegrid methods. The fundamental concept behind this method involves the use of a grid hierarchy, with a specified coarsening ratio. At each grid level, a two-step process is implemented: first, smoothing is performed to improve solutions, and then these solutions are approximated on a coarser grid. Classic iterative methods quickly reduce the oscillatory error modes of the finest grid in the initial iterations, but leaving the smooth modes, which makes the method lose its effectiveness [13,26]. With that, we transfer information (residue and/or solution) from the finer grid to the immediately coarser grid using restriction operators, where the smooth modes become more oscillatory and the method is known to be effective [26,27]. When reaching the coarsest possible or desired grid, the other transfers information (correction) from the coarser grid must be returned to the original finer grid of the problem, using prolongation operators. This accelerates the convergence of the method [26] because it becomes efficient for all error components (oscillatory and smooth).

Depending on the nature of the data exchange between grids, we can employ either the Correction Scheme (CS), where only the residue is transferred, or the Full Approximation Scheme (FAS), where the residue and the solution are transferred. BookBriggs2000 [25] suggest using CS for linear problems and FAS for nonlinear ones. The specific order in which the grids are gone through defines the type of multigrid cycle, such as V, W, or F, among others. We use the W-cycle because it is more robust [26].

We define the smoothing numbers in the restriction (ν_1) and prolongation (ν_2) process, respectively to be the pre- and post-smoothing numbers of the solver. Furthermore, we use standard coarsening $cr = 2$, *i.e.* the coarsening ratio with $H = 2h$ [26,27], where h and H are the distances between the consecutive points of the fine and the coarse grid, respectively.

Figure 1 depicts a W-cycle for the case of $l = 5$ grid coarsening levels. Algorithm 1 is based on the W-cycle for the CS-scheme considering $l > 1$ grid levels, where I_h^{2h} and I_{2h}^h are, respectively, the restriction and prolongation operators. In this case, $L_{\max}$ means the maximum number of levels. In both Figure 1 and Algorithm 1, the standard coarsening is considered.

Algorithm 1 MG-W-cycle (l)

if $l = L_{\max}$ (coarsest grid level) **then**
  Solve $A^l v^{(l)} = f^{(l)}$ in coarse grid $\Omega^{2^{l-1}h}$.
else
  Smooth ν_1 times $A^l v^{(l)} = f^{(l)}$ on grid $\Omega^{2^{l-1}h}$.
  Calculate and restrict the residual: $f^{(l+1)} = I_{2^{l-1}h}^{2^l h}(f^{(l)} - A_l v^{(l)})$.
  for *cycle* $= 1 : 2$ **do**
    Solve in the next level: **MG-*W*-cycle**$(l+1)$.
  end for
  Correct using prolongation: $v^{(l)} \leftarrow v^{(l)} + I_{2^l h}^{2^{l-1}h} v^{(l+1)}$.
  Smooth ν_2 times $A^l v^{(l)} = f^{(l)}$ on grid $\Omega^{2^{l-1}h}$.
end if

In this work, the process of transferring information from the fine grid to the coarser grid (restriction) will be done using the full-weighting operator and the of transferring information from the coarse grid to the finer grid (prolongation) will be done using linear (one-dimensional case) or bilinear (two-dimensional case) interpolation operator, defined by [26,27].

4. A discretization scheme with RRE

4.1. Discretization error

The difference between the exact analytical solution ($\overline{\phi}$) and the numerical solution (ϕ) of a variable of interest is called numerical error (E) [41]. E can result from various sources, described in Art_Marchi2002 [42] as truncation errors (E_T), iteration errors (E_I), and rounding errors (E_π). When E_I and E_π are minimized or even nonexistent, E_T is referred to as discretization error (E_h) [41].

E_h can be represented based on the Taylor series by

$$E_h = E(\phi) = c_0 h^{p_0} + c_1 h^{p_1} + c_2 h^{p_2} + \ldots \sum_{V=0}^{\infty} c_V h^{p_V}, \tag{15}$$

where the coefficients $c_0, c_1, c_2, \ldots$ are real numbers and can be functions of the dependent variable and its derivatives but are independent of h.

The exponents $p_0, p_1, p_2, \ldots$ are the true orders of E_h, and their set is represented as $p_V = \{p_0, p_1, p_2, \ldots\}$, with its elements being positive integers usually following the relationship $1 \leq p_0 < p_1 < \ldots$ characterizing an arithmetic progression. The first element of p_V, p_0, is referred to as the asymptotic order.

The analysis of p_0 a *posteriori* of the numerical solution is based on the calculation of the effective orders p_E when the analytical solution is known or apparent orders p_U otherwise. Their expressions are given by [43]

$$p_E = \frac{\log\left(\frac{E_{h_1}}{E_{h_2}}\right)}{\log(r)}, \tag{16}$$

and

$$p_U = \frac{\log\left(\frac{\phi_2 - \phi_1}{\phi_3 - \phi_2}\right)}{\log(r)}, \tag{17}$$

where ϕ_1, ϕ_2 and ϕ_3 correspond, respectively, to the numerical solutions for a specific variable of interest on the grids Ω^{h_1} (coarse), Ω^{h_2} (fine), and Ω^{h_3} (superfine), with grid spacings h_1, h_2 and h_3, E_{h_i} is the discretization error associated with the grid Ω^{h_i}, and $r = h_1/h_2 = h_2/h_3$ is the refinement ratio for the grids.

4.2. Repeated Richardson extrapolation

The Richardson Extrapolation (RE) is given by [4]:

$$\phi_\infty = \phi_{g+1} + \frac{\phi_{g+1} - \phi_g}{r^{p_0} - 1}, \tag{18}$$

where ϕ_∞ is the estimated analytical solution, ϕ_{g+1} and ϕ_g are the numerical solutions on the fine and coarse grids, respectively, and $r = \frac{h_g}{h_{g+1}}$ is the refinement ratio. This expression will be effective if ϕ_g exclusively contains discretization errors.

The Repeated Richardson Extrapolation (RRE) consists of the recursive application of RE with the aim of increasing the level of accuracy of numerical solutions. The recursive process is created from Eq. (18), which is presented in Art_Marchi_Novak2013 [10] as

$$\phi_{g,m} = \phi_{g,m-1} + \frac{\phi_{g,m-1} - \phi_{g-1,m-1}}{r^{p_{m-1}} - 1}, \tag{19}$$

where m represents the extrapolation level, and g corresponds to the grid level, with $m = 1, 2, \ldots$ e $g = m+1, m+2 \ldots.$

From a theoretical standpoint, Eq. (19) can be repeated infinitely. However, for practical applications, a limit value is considered for $g = G$, where G is a positive integer corresponding to the number of grids used. It is assumed that the use of this recursive process given by Eq. (19) progressively increases the order of accuracy of E_h [5].

An analysis of the resulting order of accuracy can be conducted by considering a generalization of p_E and p_U for RRE, as described in Art_Marchi2013 [43]:

$$(p_E)_{g,m} = \frac{\log\left(\frac{E_{h_{g-1},m}}{E_{h_g,m}}\right)}{\log(r)}, \tag{20}$$

and

$$(p_U)_{g,m} = \frac{\log\left(\frac{\phi_{g-1,m} - \phi_{g-2,m}}{\phi_{g,m} - \phi_{g-1,m}}\right)}{\log(r)}, \tag{21}$$

where $g = 2, \ldots, G$ and $m = 1, \ldots, g-1$ for Eq. (20); and $g = 3, \ldots, G$ and $m = 1, \ldots, \mathrm{Int}((g-3)/2)$ for Eq. (21), where $\mathrm{Int}(\beta)$ corresponds to the integer part of the real number β. In this perspective, when the analytical solution is not known, and even the true orders are unknown, the calculation of RRE can be performed by considering the values of $(p_U)_{g,m-1}$ instead of p_{m-1} in Eq. (19).

A schematic representation of the use of RRE is presented in Table 1. When $m = 0$, there is the numerical solution ϕ without any extrapolation. For $m = 1$, there is one level of extrapolation, for $m = 2$, there are two levels of extrapolations, and so on, up to the maximum allowed value for m in the grid Ω^{h_g}, which is $m = G - 1$. Theoretically, $\phi_{G,G-1}$ represents the numerical solution with the highest level of accuracy among all $\phi_{g,m}$.

When analyzing Table 1, it is evident that for each obtained value of $\phi_{m,g}$, the numerical solution in at least two distinct grids (g and $g-1$) is required, considering p_E. Therefore, when

Table 1. Schematic representation of the use of RRE.

$m=0$		$m=1$		$m=2$	$\cdots$	$m=G-2$		$m=G-1$
$\phi_{1,0}=\phi_1$								
$\phi_{2,0}=\phi_2$	$\searrow$ $\rightarrow$	$\boxed{\phi_{2,1}}$						
$\phi_{3,0}=\phi_3$		$\phi_{3,1}$	$\searrow$ $\rightarrow$	$\boxed{\phi_{3,2}}$				
$\vdots$		$\vdots$		$\vdots$	$\ddots$			
$\phi_{G-1,0}=\phi_{G-1}$		$\phi_{G-1,1}$		$\phi_{G-1,2}$	$\cdots$	$\boxed{\phi_{G-1,G-2}}$		
$\phi_{G,0}=\phi_G$		$\phi_{G,1}$		$\phi_{G,2}$	$\cdots$	$\phi_{G,G-2}$	$\searrow$ $\rightarrow$	$\boxed{\phi_{G,G-1}}$

using p_U (where the exact solution $\overline{\phi}$ is not known), at least three distinct grids ($g, g-1$ and $g-2$) are required, according to Eq. (21).

Remark 2. The RRE is a post-processing technique used to decrease the discretization error of numerical solutions without increasing the number of terms obtained by the Taylor series, it depends only on the collected data. Therefore, there is no problem in taking a simple domain with a discretization in simple meshes. As the RRE is a post-processing, its application is independent of how data were collected. In the present work, we adopt the standard geometric multigrid, that is usually recommended to orthogonal and non-orthogonal structured grids. However, for unstructured grids, the algebric multigrid can be applied.

5. Error analysis

5.1. Estimates for the discretization error

When calculating the difference between the estimated analytical solution (ϕ_∞) for a given variable of interest and its numerical solution (ϕ), an estimate for the numerical error is obtained [44], that is,

$$U(\phi) = \phi_\infty - \phi. \tag{22}$$

Estimators for the discretization error will be described below, taking into account the use of RRE.

5.1.1. Corrected Richardson estimator (pmc)

The Richardson estimator (U_{pm}) is introduced by Art_Marchi2013 [43] as:

$$U_{pm}(\phi_{g,m}) = \frac{\phi_{g,m} - \phi_{g-1,m}}{r^{p_m} - 1}, \tag{23}$$

where g represents the grid level, and m represents the extrapolation level, valid for $m = [0, G-2]$ and $g = [m+2, G]$, and p_m corresponds to the values of p_V. Observing Eq. (23), it is evident that the U_{pm} estimator is not suitable for estimating the discretization error associated with $\phi_M = \{\phi_{2,1}, \phi_{3,2}, \ldots, \phi_{g,g-1}, \ldots, \phi_{G,G-1}\}$. Its application is intended for solutions with one level less of extrapolation $\{\phi_{2,0}, \phi_{3,1}, \ldots, \phi_{g,g-2}, \ldots, \phi_{G,G-2}\}$, that is, $m = g-2$. Alternatively, Art_Marchi2016 [5] proposed the use of a correction factor r^{pm}, and thus, the estimator becomes

$$U_{pmc}(\phi_{g,m}) = r^{p_m} U_{pm}(\phi_{g+1,m}), \tag{24}$$

where $m = g - 1$. U_{pmc} is called the corrected pm estimator, and the error estimate will be denoted as E_m.

5.1.2. ψ^* Estimator

When considering the numerical solutions for the last extrapolation level with the maximum m, ϕ_M, the estimator ψ is employed by considering the convergence ratio of ϕ_M and estimating E_m as follows:

$$U_\psi(\phi_{g,m}) = \frac{\phi_{g,m} - \phi_{g-1,m-1}}{\psi - 1}, \tag{25}$$

where

$$\psi = (\psi_M)_g = \frac{\phi_{g-1,m-1} - \phi_{g-2,m-2}}{\phi_{g,m} - \phi_{g-1,m-1}}, \tag{26}$$

for $g = 3, \ldots, G$.

The use of U_ψ will only be effective if $|\psi| > 1$, leading to the convergence of ϕ_M and, consequently, reducing the magnitude of E_m [42]. A correction to Eq. (25), according to Art_Marchi2016 [5], is given by:

$$\psi^* = \begin{cases} \dfrac{\phi_{g,m} - \phi_{g-1,m-1}}{\phi_{g+1,m+1} - \phi_{g,m}}, & g = 2, 3, \ldots, G-1 \\ \dfrac{(\phi_{g-1,m-1} - \phi_{g-2,m-2})^2}{(\phi_{g,m} - \phi_{g-1,m-1})(\phi_{g-2,m-2} - \phi_{g-3,m-3})}, & g = G \end{cases}. \tag{27}$$

Thus, the calculation of the numerical error estimate associated with ϕ_M becomes:

$$U_{\psi^*}(\phi_{g,m}) = \frac{\phi_{g,m} - \phi_{g-1,m-1}}{\psi^* - 1}, \tag{28}$$

for $g = 2, \ldots, G$.

5.2. Effectiveness of an error estimate

The effectiveness $(\Theta(U))$ of an estimate U for the numerical error E can be generally assessed using the calculation provided in Art_Zhu1990 [45]:

$$\Theta(U) = \frac{U}{E}. \tag{29}$$

Given Eq. (29), an estimate U will be accurate when $\Theta(U) \approx 1$ and reliable when $\Theta(U) \geq 1$.

Remark 3. Using the RRE method, we achieve high accuracy with reduced computational cost. This allows us to solve problems with the desired precision on meshes that do not need to be highly refined or, alternatively, to achieve greater precision on existing meshes. Additionally, having good estimators, calibrated with analytical solutions, is crucial. These estimators significantly aid in solving problems for which there are no known analytical solutions available, providing a robust and efficient approach for a wide range of problems.

6. Results

The use of the RRE requires obtaining numerical solutions for a specific variable of interest on a collection of distinct grids. In this work, the variables of interest are located at predefined

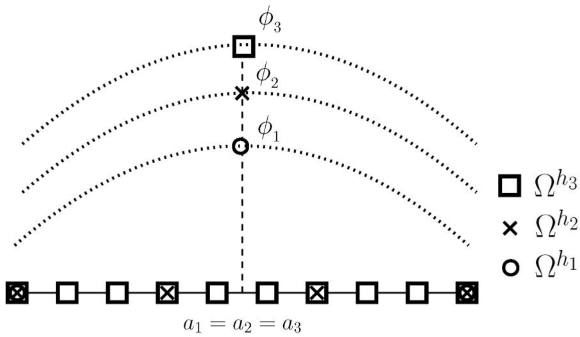

Figure 2. Variable with a pre-established location, located at the midpoint between nodal points in different grids.

Table 2. Input parameters for the problem.

Symbol	Quantity	Value	Unit
λ_w	Fluid mobility in phase *w*	1	$(Pas)^{-1}$
λ_n	Fluid mobility in phase *n*	2	$(Pas)^{-1}$
ρ_w	Density of fluid in phase *w*	1	kg/m^3
ρ_n	Density of fluid in phase *n*	2	kg/m^3

positions, located at the midpoint between nodal points on different grids. Figure 2 (adapted from Art_Marchi2016 [5]) illustrates the behavior of this type of variable in relation to the grid refinement process. In this figure, we have ϕ_1 with coordinate a_1, ϕ_2 with coordinate a_2, and ϕ_3 with coordinate a_3, corresponding respectively to the numerical solutions obtained on grids Ω^{h_1} (coarse), Ω^{h_2} (fine), and Ω^{h_3} (superfine), with a constant refinement ratio $r = h_1/h_2 = h_2/h_3$.

For these variables, the location of the variable of interest does not coincide with the nodal coordinates, making it necessary to use a method that allows its calculation before applying the RRE. The most suitable technique for this purpose, based on the obtained nodal values, is linear interpolation [46]. The result of linear interpolation can be attributed to the location of the variable of interest ϕ, and from these values obtained for ϕ, we apply the RRE with Eq. (19).

Remark 4. In the context of the scientific literature involving RRE, Art_Marchi2016 [5] presented and tested a novel numerical procedure for reducing the discretization error of variables for which RRE performs poorly. In Figure 2 by Art_Marchi2016 [5], five types of variables determined by their locations on different grids are illustrated. The location of a variable can be changed through grid refinement. In that paper, for the five types, RRE was analyzed in the problems of the 1D Poisson equation, 2D Burgers equations, and 2D Navier–Stokes equations. In this study, we examine a variable with a pre-established location, positioned at the midpoint between nodal points on different grids (type II variable described in Art_Marchi2016 [5]).

Based on the methodology described in Section 4.2, we present the results obtained with the use of the RRE. All simulations were executed in MATLAB R2021a. As the stopping criterion for the linearization process, we used the maximum absolute value of pressure corrections, i.e. max $(|\delta p_w|, |\delta p_n|) \leq TOL$. For the iterative process, we employed the infinity norm of the residual, dimensionless by the initial estimate. That is, $||r^k||_\infty/||r^0||_\infty \leq TOL$, where r^k represents the residual at iteration k, r^0 is the residual at the initial estimate, and TOL is the tolerance adopted until reaching the double-precision rounding error, ensuring the minimization of iteration and rounding error sources. We utilized the multigrid method with the following components: *CS* scheme, W-cycle, standard coarsening ratio, Gauss-Seidel smoother, full weighting restriction operator, and linear interpolation prolongation operator.

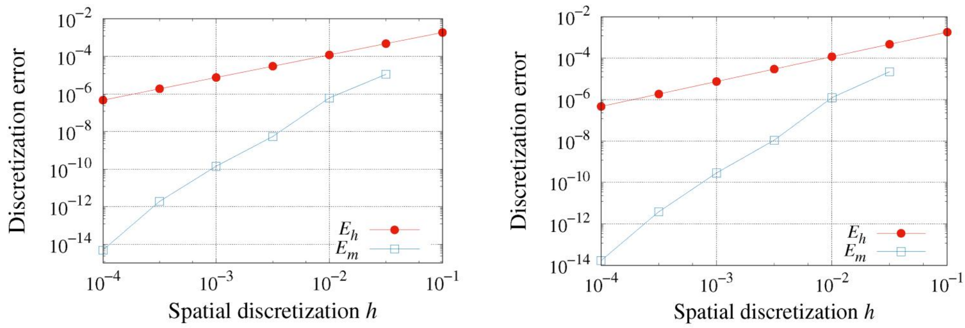

(a) Variable p_n. (b) Variable p_w.

Figure 3. Discretization error considering $\Phi = 0.4$, with and without the use of RRE for variables: (a) p_n e (b) p_w.

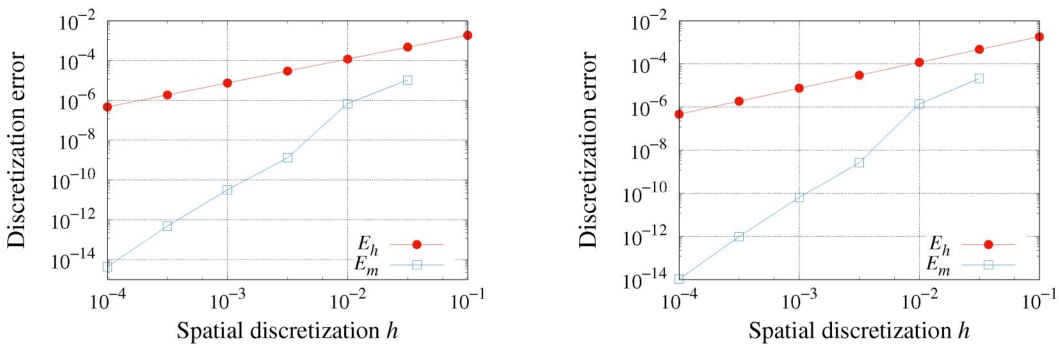

(a) Variable p_n. (b) Variable p_w.

Figure 4. Discretization error considering $\Phi = 0.9$, with and without the use of RRE for variables: (a) p_n e (b) p_w.

6.1. Results to the one dimensional case

We present the results for the p_n and p_w variables for porosities $\Phi = 0.4$ and 0.9, with a permeability of $K = 10^{-2}\ m^2$. The coarsest grid considered had $N = 4$ volumes, while the finest had $N = 256$ volumes, resulting in a total of $G = 7$ grids. To simulate the problem, we used the parameters employed by Thesis_Illiano2016 [36], which are presented in Table 2.

When conducting a comparative analysis of the discretization error curves associated with the variables p_n and p_w, both without the use of RRE (E_h) and with its application (E_m), as illustrated in Figures 3-4, for porosity values $\Phi = 0.4$ and $\Phi = 0.9$, respectively, the effectiveness of using RRE in minimizing the discretization error is evident. In other words, the application of RRE results in a significant reduction in E_m compared to E_h.

The results presented in Tables 3 and 4, respectively for the variables p_n and p_w, provide an example of the effect of RRE on reducing E_h, for $\Phi = 0.4$, which were evaluated by calculating the ratio $|E_h|/|E_m|$. Similar numerical results were observed for $\Phi = 0.9$. For instance, in the grid with 256 volumes, applying six levels of RRE reduced the error for the variable p_w by more than 27 million times, and for the variable p_n, this reduction was over 96 million times.

The orders of accuracy for the variable p_n without the application of RRE ($m = 0$) and with the application of RRE can be observed in Table 5. For two levels of extrapolation ($m = 2$), as an example, the value of p_E approaches 4 with grid refinement.

It can also be noticed that, as the grid refinement, $h \to 0$, the values of p_E for each level of extrapolation tend to form an arithmetic progression, consistent with theoretical results available in the literature [43].

Table 3. Reduction of the error in three different grids, variable p_n considering $\Phi = 0.4$.

grid h	32 volumes	64 volumes	256 volumes
m	3	4	6
$\|E_h\|$	3.0038E-05	7.5139E-06	4.6978E-07
$\|E_m\|$	5.4271E-09	1.4134E-10	4.8652E-15
$\|E_h\|/\|E_m\|$	5.5348E + 03	5.3162E + 04	9.6558E + 07

Table 4. Reduction of the error in three different grids, variable p_w considering $\Phi = 0.4$.

grid h	32 volumes	64 volumes	256 volumes
m	3	4	6
$\|E_h\|$	2.9558E-05	7.3984E-06	4.6272E-07
$\|E_m\|$	1.0854E-08	2.8269E-10	1.6720E-14
$\|E_h\|/\|E_m\|$	2.7232E + 03	2.6172E + 04	2.7675E + 07

Table 5. Effective order of p_E for the variable p_n considering $\Phi = 0.4$.

h	$m = 0$	$m = 1$	$m = 2$	$m = 3$	$m = 4$	$m = 5$
1.2500E-01	1.9748					
6.2500E-02	1.9924	3.7174				
3.1250E-02	1.9976	3.6547	3.8207			
1.5625E-02	1.9991	3.4948	3.9838	7.3758		
7.8125E-03	1.9996	3.3316	3.9945	5.5625	8.6979	
3.9062E-03	1.9998	3.2001	3.9967	4.7335	6.2330	7.5683

Table 6 presents the results for the calculation of effectiveness $\left(\Theta = \frac{U}{E}\right)$, for variables p_n and p_w, obtained for the estimators U_{ψ^*} and U_{pmc}. It can be observed that, for these variables, both estimators proved to be accurate, with U_{pmc} being the more reliable estimator. Figure 5 illustrates the results for E_h, E_m and its U_{pmc} estimate.

6.2. Extension to the two-dimensional case

For the two-dimensional case, we consider a test problem with analytical solution proposed by Thesis_Kvashchuk2015 [47]. In that work, Kvashchuk considered the mixed pressure-saturation formulation $(\overline{p}, S_w)$, where $\overline{p} = \frac{p_w + p_n}{2}$ and used the analytical solution

$$\overline{p}(\mathbf{x}, t) = tx(1-x)y(1-y), \tag{30}$$

$$S_w(\mathbf{x}, t) = \frac{1}{2} + tx(1-x)y(1-y), \tag{31}$$

defined in the spatial-temporal domain $\Omega \times I = [0,1] \times [0,1] \times [0,1]$, with initial and Dirichlet boundary conditions given by analytical solutions (Eqs. 30 and 31). For reasons analogous to those explained in Section 2.1, adaptations are also made to the pressure-saturation formulation, resulting in a system with the variables p_w and p_n, using Eqs. (6) and (7) for the two-dimensional case.

To simulate this two-dimensional problem, we used the parameters employed by [47], which are presented in Table 7.

We present the results for the p_n and p_w variables. The coarsest grid considered had $N_x \times N_y = 10 \times 10$ volumes, while the finest had $N_x \times N_y = 320 \times 320$, resulting in a total of $G = 6$ grids.

The results presented in Table 8, for the variables p_n and p_w, provide an example of the effect of RRE on reducing E_h, which were evaluated by calculating the ratio $|E_h|/|E_m|$. For instance, in

Table 6. Effectiveness of the estimators U_{ψ^*} and U_{pmc} for the variables p_n and p_w considering $\Phi = 0.4$ for E_m.

	Variable p_n		Variable p_w	
h	U_{ψ^*}/E_m	U_{pmc}/E_m	U_{ψ^*}/E_m	U_{pmc}/E_m
1.2500E-01	1.0625E + 00	1.0559E + 00	1.06995E + 00	1.05597E + 00
6.2500E-02	9.4169E-01	9.9117E-01	9.41698E-01	9.91178E-01
3.1250E-02	1.0354E + 00	1.0260E + 00	1.03550E + 00	1.02604E + 00
1.5625E-02	9.8801E-01	1.0134E + 00	9.88058E-01	1.01347E + 00
7.8125E-03	9.8942E-01	1.0025E + 00	9.91151E-01	1.00438E + 00
3.9062E-03	8.6005E-01	8.6194E-01	1.60188E + 00	1.61317E + 00

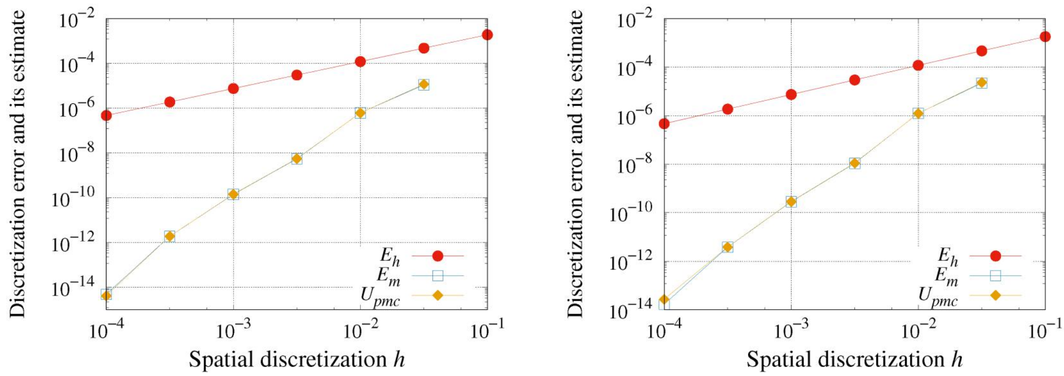

(a) Variable p_n. (b) Variable p_w.

Figure 5. Discretization error without the use of RRE (E_h), with the use of RRE (E_m), and its estimate U_{pmc} × spatial discretization h, considering $\Phi = 0.4$, for the variables: (a) p_n and (b) p_w.

Table 7. Input parameters for the two-dimensional problem.

Symbol	Quantity	Value	Unit
λ_w	Fluid mobility in phase w	$\frac{1}{4}$	$(Pa\ s)^{-1}$
λ_n	Fluid mobility in phase n	$\frac{3}{4}$	$(Pa\ s)^{-1}$
ρ_w	Density of fluid in phase w	1	kg/m^3
ρ_n	Density of fluid in phase n	1	kg/m^3
K	Permeability	1	m^2
Φ	Porosity	1	

the grid with $N_x \times N_y = 320 \times 320$ volumes, applying five levels of RRE reduced the error for the variable p_w by more than 159 million times.

Table 9 presents the results for the calculation of effectiveness for variable p_w, obtained for the estimators U_{ψ^*} and U_{pmc}. It is noted that the estimator $U_{p_{mc}}$ is the most accurate and reliable. For the variable p_n, the numerical results are similar.

Figure 6 illustrates the discretization errors and its estimate $U_{p_{mc}}$, for the variables p_n and p_w. This figure show the behavior of the discretization error without (E_h) and with (E_m) the use of RRE, highlighting the significant difference in their magnitudes. For this problem, considering the grid $N = 160 \times 160$, Thesis_Kvashchuk2015 [47] and Art_Oliveira2024 [15] obtained an approximate error of the order of 1.0E-06. With a similar computational cost, in this paper, we achieved an error of the order of 1.0E-12 on the same grid. Regarding the estimator, there is an agreement between E_m and $U_{p_{mc}}$, indicating that is accurate and reliable. Thus, their use represents an alternative for the numerical verification of problems for which the analytical solution is not known.

We also evaluate the multigrid method complexity using geometric adjustment of the type [37]

Table 8. Reduction of the error in two different grids, variables p_n and p_w for the two-dimensional problem.

	variable p_n		variable p_w	
$N_x \times N_y$	40×40	320×320	40×40	320×320
m	2	5	2	5
$\|E_h\|$	1.1062E-05	1.7261E-07	7.5699E-05	1.1835E-06
$\|E_m\|$	1.9909E-08	5.3734E-15	1.6265E-07	7.4036E-15
$\|E_h\|/\|E_m\|$	5.5561E + 02	3.2124E + 07	4.6540E + 02	1.5985E + 08

Table 9. Effectiveness of the estimators U_{ψ^*} and $U_{p_{mc}}$ for the variable p_w, for the two-dimensional problem.

h	U_{ψ^*}/E_m	$U_{p_{mc}}/E_m$
5.0000E-02	1.070609E + 00	1.068340E + 00
2.5000E-02	9.386907E-01	9.986569E-01
1.2500E-02	1.016404E + 00	1.015017E + 00
6.2500E-03	9.832290E-01	9.977431E-01
3.1250E-03	1.975099E + 00	1.966314E + 00

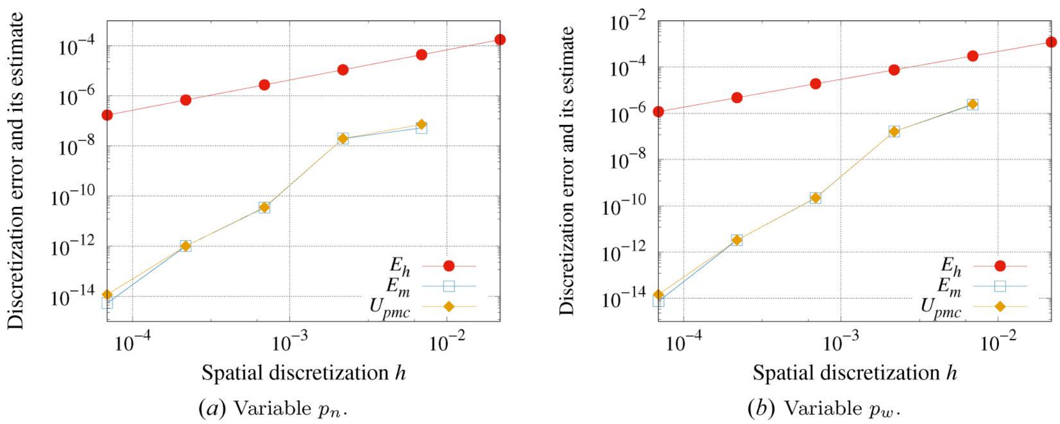

Figure 6. Discretization error without the use of RRE (E_h), with the use of RRE (E_m), and its estimator $U_{p_{mc}}$ × spatial discretization h for the two-dimensional problem, for the variables: (a) p_n and (b) p_w.

$$t_{CPU} = c(N)^p, \tag{32}$$

where c represents the method coefficient, p corresponds to the order of complexity and N is the total number of unknowns in the problem. According to reference studies [26,27], the multigrid method is considered ideal when the order of complexity p approaches unity and c tends to zero. To show the optimality of the proposed solver, we considered the relative CPU time in terms of the number of unknowns (in the first time step and the first linearization) on different grids, $N = 10 \times 10,\ 20 \times 20,\ 40 \times 40,\ \cdots,\ 320 \times 320$, and we obtained $c = 0.0018$ and $p = 1.0863$. We can see that the computational cost of the solver is close to $\mathcal{O}(N)$ which is in accordance with the literature [15,26].

7. Conclusions

In this work, we evaluated the efficiency of the RRE applied to the variables p_n and p_w of the two-phase flow problem in porous media, aiming to minimize and estimate E_h, and, increase the accuracy of numerical solutions. We found that: (1) the use of RRE was effective in terms of improving the accuracy of numerical solutions; (2) concerning the estimates of numerical error, considering the solutions obtained with the application of RRE, the corrected Richardson estimator U_{pmc} is recommended to provide better precision and reliability compared to other analyzed estimator.

Acknowledgments

The first author would like to express gratitude to the State University of Centro-Oeste (UNICENTRO) for providing financial support and a full-time PhD study license. The authors also extend their thanks to the Graduate Program in Numerical Methods in Engineering (PPGMNE) at the Federal University of Paraná (UFPR).

Disclosure statement

The authors report there are no competing interests to declare.

ORCID

Marcelo Henrique Sabatini http://orcid.org/0009-0000-8721-5976
Marcio Augusto Villela Pinto http://orcid.org/0000-0003-4166-4674
Marcio André Martins http://orcid.org/0000-0002-7094-1215
Michely Laís de Oliveira http://orcid.org/0000-0002-0646-9817
Sandro Rodrigues http://orcid.org/0000-0003-3071-8550

References

[1] A. Huerta, A. Angeloski, X. Roca and J. Peraire, "Efficiency of high-order elements for continuous and discontinuous Galerkin methods," *Numer. Meth. Eng.*, vol. 96, no. 9, pp. 529–560, 2013. DOI: 10.1002/nme.4547.

[2] N. Tonicello and I. Matthias, "A high-order diffused-interface approach for two-phase compressible flow simulations using a discontinuous Galerkin framework," *J. Computat. Phys.*, vol. 508, pp. 112983, 2024. DOI: 10.1016/j.jcp.2024.112983.

[3] L. F. Richardson and J. A. Gaunt, "The deferred approach to the limit," *Philosoph. Trans. Roy. Soc. London*, vol. 226, pp. 299–361, 1927. DOI: 10.1098/rsta.1927.0008.

[4] G. Dahlquist and A. Bjorck, *Numerical Methods in Scientific Computing*. Philadelphia: SIAM, 2008.

[5] C. H. Marchi, *et al.*, "Polynomial interpolation with repeated Richardson extrapolation to reduce discretization error in CFD," *Appl. Math. Modelling*, vol. 40, no. 21-22, pp. 8872–8885, 2016. DOI: 10.1016/j.apm.2016.05.029.

[6] C. H. Marchi, F. F. Giacomini and C. D. Santiago, "Repeated Richardson extrapolation to reduce the field discretization error in computational fluid dynamics," *Numer. Heat Transfer, B. Fundamentals*, vol. 70, no. 4, pp. 340–353, 2016b. DOI: 10.1080/10407790.2016.1215702.

[7] E. Erturk, T. C. Corke and C. Gökçöl, "Numerical solutions of 2D steady incompressible driven cavity flow at high Reynolds numbers," *Int. J. Numer. Meth. Fluids*, vol. 48, no. 7, pp. 747–774, 2005. DOI: 10.1002/fld.953.

[8] K. Rahul and S. N. Bhattacharyya, "One-sided finite-difference approximations suitable for use with Richardson extrapolation," *J. Computat. Phys.*, vol. 219, no. 1, pp. 13–20, 2006. DOI: 10.1016/j.jcp.2006.05.035.

[9] C. H. Marchi and E. M. Germer, "Effect of ten CFD numerical schemes on repeated Richardson extrapolation (RRE)," *J. Appl. Computat. Math.*, vol. 2, no. 128, pp. 1–8, 2013. DOI: 10.4172/2168-9679.1000128.

[10] C. H. Marchi, L. A. Novak, C. D. Santiago and A. P. S. Vargas, "Highly accurate numerical solutions with repeated Richardson extrapolation for 2D laplace equation," *Appl. Math. Model.*, vol. 37, no. 12-13, pp. 7386–7397, 2013b. DOI: 10.1016/j.apm.2013.02.043.

[11] T. A. AbdelMigid, K. M. Saqr, M. A. Kotb and A. A. Aboelfarag, "Revisiting the lid-driven cavity flow problem: review and new steady state benchmarking results using GPU accelerated code," *Alexandria Eng. J.*, vol. 56, no. 1, pp. 123–135, 2017. DOI: 10.1016/j.aej.2016.09.013.

[12] S. Rodrigues, M. A. V. Pinto, M. A. Martins and S. R. Franco, "Reducing the discretization error for a poroelasticity problem in variables having extreme values," *J. Braz. Soc. Mech. Sci. Eng.*, vol. 44, no. 4, pp. 1–11, 2022. DOI: 10.1007/s40430-022-03410-4.

[13] L. P. Silva, B. B. Rutyna, A. R. S. Righi and M. A. V. Pinto, “High order of accuracy for Poisson equation obtained by grouping of repeated Richardson extrapolation with fourth order schemes,” *Comput. Model. Eng. Sci.*, vol. 128, no. 2, pp. 699–715, 2021. DOI: 10.32604/cmes.2021.014239.
[14] W. Ehlers and J. Bluhm, *Porous Media: Theory, Experiments and Numerical Applications*. Berlin: Springer, 2002.
[15] M. L. Oliveira, M. A. V. Pinto, C. Rodrigo and F. J. Gaspar, “Modified Picard with multigrid method for two-phase flow problems in rigid porous media,” *Numer. Meth. Eng.*, vol. 125, no. 5, pp. 1–13, 2024. DOI: 10.1002/nme.7397.
[16] P. H. S. Slompo, M. A. V. Pinto and M. L. Oliveira, “Comparison between Van Genuchten and Brooks-Corey parameterizations in the solution of multiphase problems in rigid one-dimensional porous media,” *J. Computat. Theoret. Transport*, vol. 52, no. 6, pp. 429–451, 2023. DOI: 10.1080/23324309.2023.2287008.
[17] M. Karimi-Fard, L. J. Durlofsky and K. Aziz, “An efficient discrete-fracture model applicable for general-purpose reservoir simulators,” *SPE J*, vol. 9, no. 02, pp. 227–236, 2004. DOI: 10.2118/88812-PA.
[18] L. Wang, F. Golfier, A.-J. Tinet, W. Chen and C. Vuik, “An efficient adaptive implicit scheme with equivalent continuum approach for two-phase flow in fractured vuggy porous media,” *Adv. Water Resources*, vol. 163, pp. 104186, 2022a. DOI: 10.1016/j.advwatres.2022.104186.
[19] M. Karimi-Fard and L. J. Durlofsky, “A general gridding, discretization, and coarsening methodology for modeling flow in porous formations with discrete geological features,” *Adv. Water Resources*, vol. 96, pp. 354–372, 2016. DOI: 10.1016/j.advwatres.2016.07.019.
[20] L. Wang, Y. Wang, C. Vuik and H. Hajibeygi, “Accurate modeling and simulation of seepage in 3D heterogeneous fractured porous media with complex structures,” *Comput. Geotech.*, vol. 150, pp. 104923, 2022b. DOI: 10.1016/j.compgeo.2022.104923.
[21] P. Bastian and R. Helmig, “Efficient fully-coupled techniques for two-phase flow in porous media: parallel multigrid solution and large scale computations,” *Adv. Water Resources*, vol. 23, no. 3, pp. 199–216, 1999. DOI: 10.1016/S0309-1708(99)00014-7.
[22] B. Ataie-Ashtiani and D. Raeesi-Ardekani, “Comparison of numerical formulations for two-phase flow in porous media,” *Geotech. Geol. Eng.*, vol. 28, no. 4, pp. 373–389, 2010. DOI: 10.1007/s10706-009-9298-4.
[23] M. A. Celia and P. Binning, “A mass conservative numerical solution for two-phase flow in porous media with application to unsaturated flow,” *Water Resources Res.*, vol. 28, no. 10, pp. 2819–2828, 1992. DOI: 10.1029/92WR01488.
[24] F. J. Gaspar, F. J. Lisbona, C. W. Oosterlee and R. Wienands, “A systematic comparison of coupled and distributive smoothing in multigrid for the poroelasticity system,” *Numer. Linear Algebra App.*, vol. 11, no. 2-3, pp. 93–113, 2004. DOI: 10.1002/nla.372.
[25] W. L. Briggs, V. E. Henson and S. F. McCormick, *A Multigrid Tutorial*, 2nd ed. Philadelphia: SIAM, 2000.
[26] U. Trottenberg, C. Oosterlee and A. Schüller, *Multigrid*. San Diego: Academic Press, 2001.
[27] P. Wesseling, *An Introduction to Multigrid Methods*. Philadelphia: R.T. Edwards, Inc., 2004.
[28] S. R. Franco, F. J. Gaspar, M. A. V. Pinto and C. Rodrigo, “Multigrid method based on a space-time approach with standard coarsening for parabolic problems,” *Appl. Math. Comput.*, vol. 317, pp. 25–34, 2018. DOI: 10.1016/j.amc.2017.08.043.
[29] M. F. Malacarne, M. A. V. Pinto and S. R. Franco, “Performance of the multigrid method with time-stepping to solve 1D and 2D wave equations,” *Int. J. Comput. Methods. Eng. Sci. Mech.*, vol. 1, pp. 1–12, 2021. DOI: 10.1080/15502287.2021.1910750.
[30] F. Oliveira, S. R. Franco and M. A. V. Pinto, “The effect of multigrid parameters in a 3D heat diffusion equation,” *Int. J. Appl. Mech. Eng.*, vol. 23, no. 1, pp. 213–221, 2018. DOI: 10.1515/ijame-2018-0012.
[31] M. A. V. Pinto, C. Rodrigo, F. J. Gaspar and C. Oosterlee, “On the robustness of ILU smoothers on triangular grids,” *Appl. Numer. Math.*, vol. 106, pp. 37–52, 2016. DOI: 10.1016/j.apnum.2016.02.007.
[32] J. M. B. Oliveira, L. K. Araki, M. A. V. Pinto and S. F. T. Gonçalves, “An alternative full multigrid SIMPLEC approach for the incompressible Navier–Stokes equations,” *Numer. Heat Transfer B. Fundamentals*, vol. 83, no. 6, pp. 410–432, 2023. DOI: 10.1080/10407790.2023.2167752.
[33] C. D. Santiago, G. R. Ströher, M. A. V. Pinto and S. R. Franco, “A multigrid waveform relaxation method for solving the Pennes bioheat equation,” *Numer. Heat Transfer A: Applicat.*, vol. 83, no. 9, pp. 976–990, 2023. DOI: 10.1080/10407782.2022.2156411.
[34] S. R. Franco and M. A. V. Pinto, “A space-time multigrid method for poroelasticity equations with random hydraulic conductivity,” *Numer. Heat Transfer B. Fundamentals*, vol. 85, no. 9, pp. 1226–1235, 2023. DOI: 10.1080/10407790.2023.2262746.
[35] P. D. Zen, M. A. V. Pinto and S. R. Franco, “A multigrid waveform relaxation method for solving the nonlinear silicon problem with relaxing boundary conditions,” *Numer. Heat Transfer. B Fundamentals*. Advance online publication, pp. 1–16, 2024. DOI: 10.1080/10407790.2024.2351543.
[36] D. Illiano, “Iterative schemes for solving coupled, nonlinear flow and transport in porous media,” Master thesis, University of Bergen, Bergen, Norway, 2016.

[37] R. L. Burden, J. D. Faires and A. M. Burden, *Numerical Analysis*, 10th ed. Boston: Cengage Learning, 2015.
[38] E. Kreyszig, *Advanced Engineering Mathematics*, 10th ed. New Jersey: John Wiley and Sons, Inc., 2011.
[39] C. R. Maliska, *Transferência de Calor e Mecânica dos Fluídos Computacional*, 2nd ed. Rio de Janeiro: LTC, 2004,
[40] R. P. Fedorenko, "On the speed of convergence of an iteration process," *USSR Comput. Math. Math. Phys*, vol. 4, pp. 227, 1964.
[41] J. H. Ferziger and M. Perić, *Computational Methods for Fluid Dynamics*, 3rd ed. New York: Springer, 2002.
[42] C. H. Marchi and A. F. C. Silva, "Unidimensional numerical solution error estimation for convergent apparent order," *Numer. Heat Transfer. B*, vol. 42, no. 2, pp. 167–188, 2002. DOI: 10.1080/10407790190053888.
[43] C. H. Marchi, L. K. Araki, A. C. Alves, R. Suero, S. F. T. Gonçalves and M. A. V. Pinto, "Repeated Richardson extrapolation applied to the two-dimensional Laplace equation using triangular and square grids," *Appl. Math. Modelling*, vol. 37, no. 7, pp. 4661–4675, 2013c. DOI: 10.1016/j.apm.2012.09.071.
[44] S. C. Chapra and R. P. Canale, *Introduction to Computing for Engineers*. New York: McGraw-Hill College, 2008,
[45] J. Z. Zhu and O. C. Zienkiewicz, "Superconvergence recovery technique and a *posteriori* error estimators," *Numer. Meth Eng.*, vol. 30, no. 7, pp. 1321–1339, 1990. DOI: 10.1002/nme.1620300707.
[46] M. A. Martins, "Repeated Richardson extrapolations with polynomial interpolations to reduce and estimate the discretization error in CFD (in Portuguese)," PhD thesis, Dept. Mechanical Engineering, Federal University of Paraná, Curitiba, PR, Brazil, 2013.
[47] A. Kvashchuk, "A robust implicit scheme for two-phase flow in porous media," Master thesis, University of Bergen, Bergen, Norway, 2016.